

Supporting Information

Surfactant-Free Shape Control of Gold Nanoparticles Enabled by Unified Theoretical Framework of Nanocrystal Synthesis

Matthew A. Wall, Stefan Harmsen, Soumik Pal, Lihua Zhang, Gianluca Arianna, John R. Lombardi, Charles Michael Drain, Moritz F. Kircher*

*Corresponding Author. Email: kirchem@mskcc.org

Contents

Part I. Supplementary Figures	2
Part II. Supplementary Movies	12
Part III. Theoretical Framework	12

Part I. Supplementary Figures

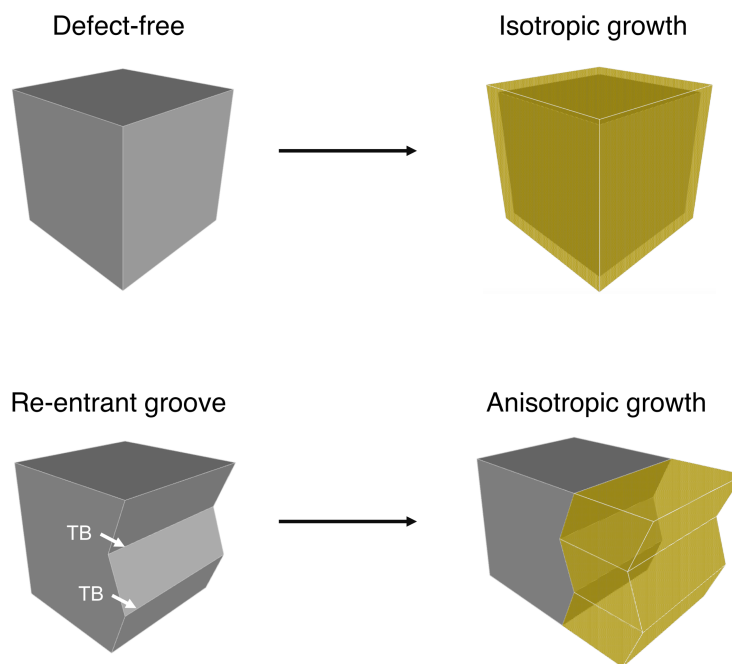


Figure S1. Re-entrant grooves drive anisotropic growth. When the surface of a nanoparticle is uniform and defect-free it will grow isotropically. However, if certain defects such as parallel twin boundaries (TB) are introduced into the surface, a locally concave surface called a re-entrant groove is created. Multiple re-entrant grooves can appear on a surface with the effect of significantly increasing the facet growth rate. One reason for this rapid growth is the catalytic effect that re-entrant grooves have on the nucleation of monolayers.

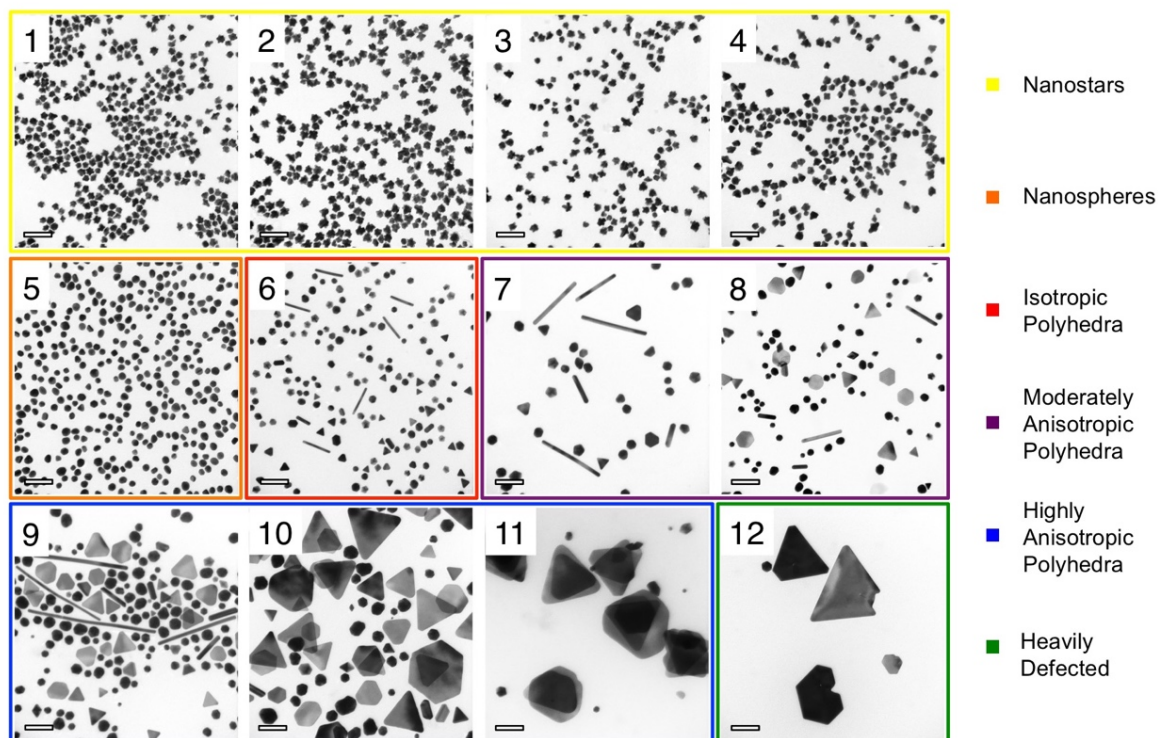


Figure S2. Changes in crystal growth as a function of growth rate. The twelve TEM images correspond to decreasing reduction rates of HAuCl_4 . All reactions have the same concentration of seeds and HAuCl_4 , such that the only synthetic variables are the amount of H_2O_2 and NaOH in solution. Panels 1 – 6 have 19.6 mM H_2O_2 and NaOH concentrations decreasing from 3.9 mM to 0.49 mM. Panels 7 – 12 have no NaOH , and H_2O_2 concentrations decreasing from 9.8×10^{-1} M to 4.9×10^{-8} M. The dominant type of products observed changes as labeled from nanostars in panel 1 to heavily defected nanoparticles in panel 12.

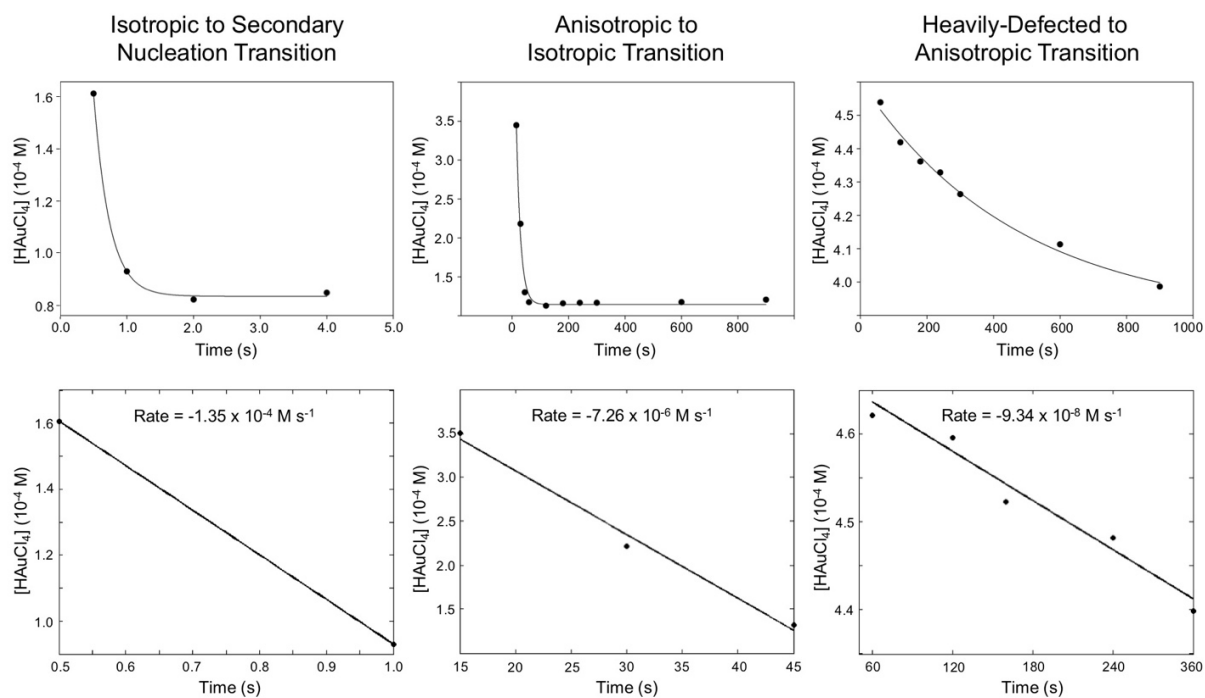


Figure S3. Kinetics of HAuCl₄ reduction. The absorbance of Au(III) was monitored by UV-visible spectroscopy at 300 nm. Representative syntheses were performed from which aliquots were removed at the measured time points and added to an equal volume of a 2 % polyvinylpyrrolidone (PVP; 10 kDa) quenching solution. All measurements, including calibration curves, were performed on the same well plate. The rates refer to the disappearance of HAuCl₄ over time.















Product	Seed	Reduction Rate
		$\geq 1.4 \times 10^{-4} \text{ M s}^{-1}$
		$\geq 1.4 \times 10^{-4} \text{ M s}^{-1}$
		$\geq 1.4 \times 10^{-4} \text{ M s}^{-1}$
		$\geq 7.3 \times 10^{-6} \text{ M s}^{-1}$ $\leq 1.4 \times 10^{-4} \text{ M s}^{-1}$
		$\geq 7.3 \times 10^{-6} \text{ M s}^{-1}$ $\leq 1.4 \times 10^{-4} \text{ M s}^{-1}$
		$\geq 9.3 \times 10^{-8} \text{ M s}^{-1}$ $\leq 7.3 \times 10^{-6} \text{ M s}^{-1}$
		$\geq 9.3 \times 10^{-8} \text{ M s}^{-1}$ $\leq 7.3 \times 10^{-6} \text{ M s}^{-1}$

Figure S4. Criteria for shape control in surfactant-free syntheses. Each product morphology forms from one or more corresponding seeds. All types of seeds (e.g. icosahedral, five-fold twinned, plate-like, etc.) can grow into spheres and stars if the reduction rate of HAuCl_4^- is sufficiently fast. The polyhedral shapes (e.g. icosahedra, decahedra, rods, plates) can only be formed in high yield if the unique corresponding seed is present in high yield. Nanorod formation has the additional requirement that the seed possess re-entrant grooves (highlighted in red on five-fold seed) on the $\{111\}$ facets. The reduction rates necessary to synthesize each shape are given in the last column.

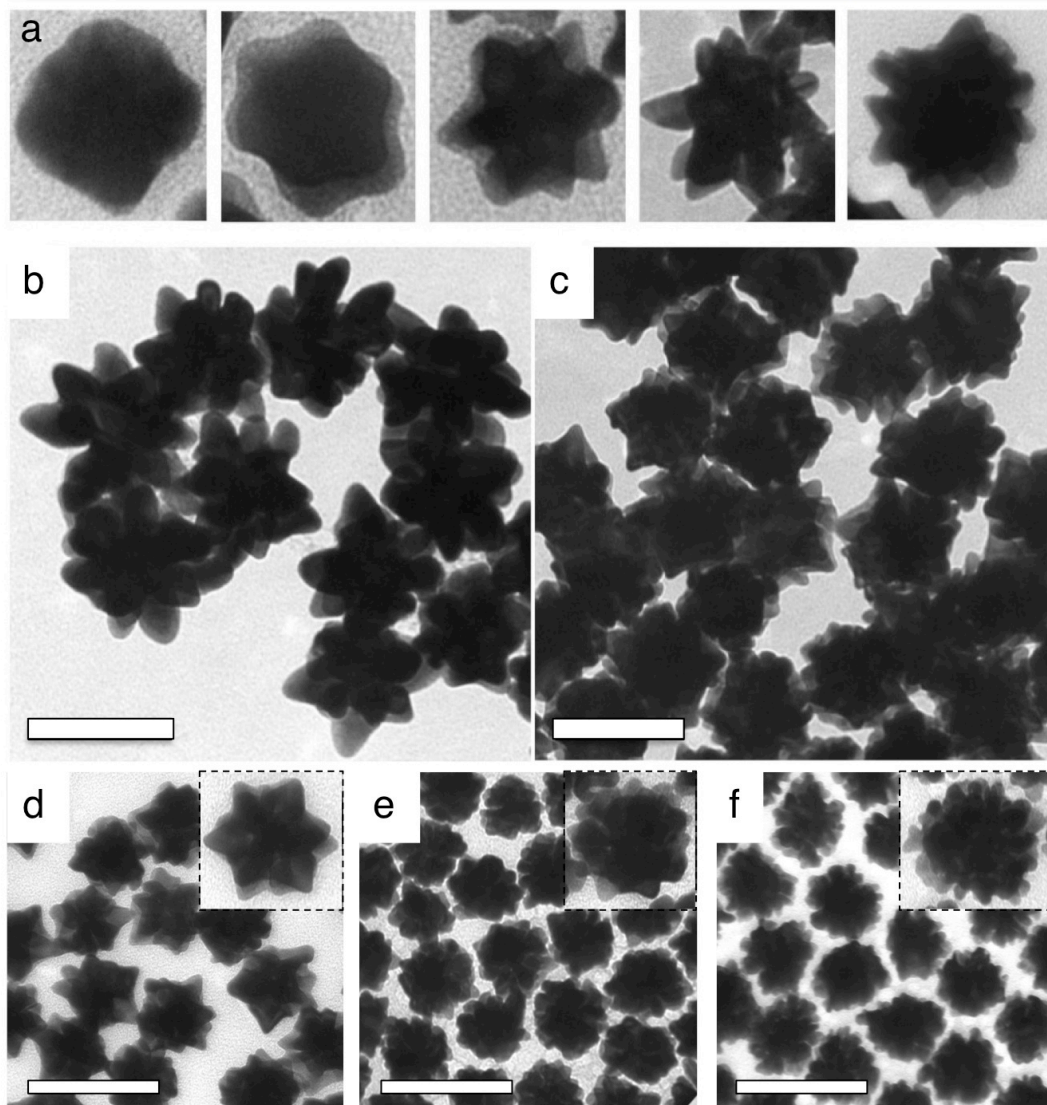


Figure S5. Tunability of nanostars. **a**, As the HAuCl_4 reduction kinetics increase, protrusions begin to grow outward from the nanoparticle core. The aspect ratio of the protrusions increases until an optimum is reached, beyond which the aspect ratio decreases and the number of protrusions increases. **b**, TEM image of characteristic nanostars formed under the minimal reaction rate sufficient to produce stable nanostars in high yield (1.0 mM/s). **c**, TEM image of characteristic nanostars formed under the fastest reaction kinetics tested shows that the number of protrusions increases and their aspect ratio decreases relative to the nanostars formed under slower kinetics. **d-f**, Nanostars grown from different seed diameters. The average number of protrusions per particle increases while maintaining the same total diameter as the seed size is increased from **(d)** 5 nm, to **(e)** 15 nm, to **(f)** 33 nm. Scale bars are 50 nm in b-c, and 100 nm in d-f.

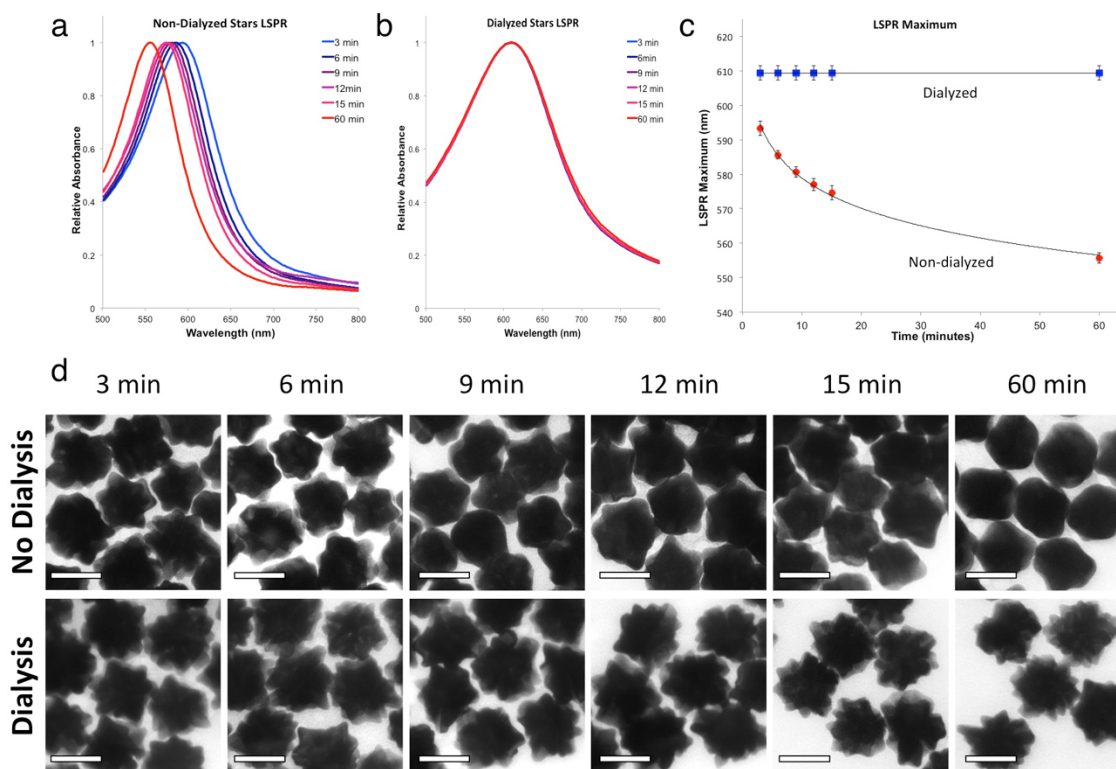


Figure S6. Nanostar transformation and stabilization. **a**, Absorbance spectra of as-synthesized gold nanostars that were not subjected to post-processing measured at the indicated time points. **b**, Absorbance spectra of as-synthesized gold nanostars that were immediately dialyzed to remove residual reagents measured at the indicated time points. **c**, Localized surface plasmon resonance (LSPR) maximum plotted against time. No shift was observed for the dialyzed gold nanostars, while the absorbance maximum of non-dialyzed gold nanostars rapidly red-shifted over time approaching 540 nm (LSPR of spherical gold nanoparticles). **d**, TEM images demonstrated spherical transformation of the non-dialyzed gold nanostars over time, while the star-shape of the dialyzed gold nanostars was preserved. Scale bars are 50 nm.

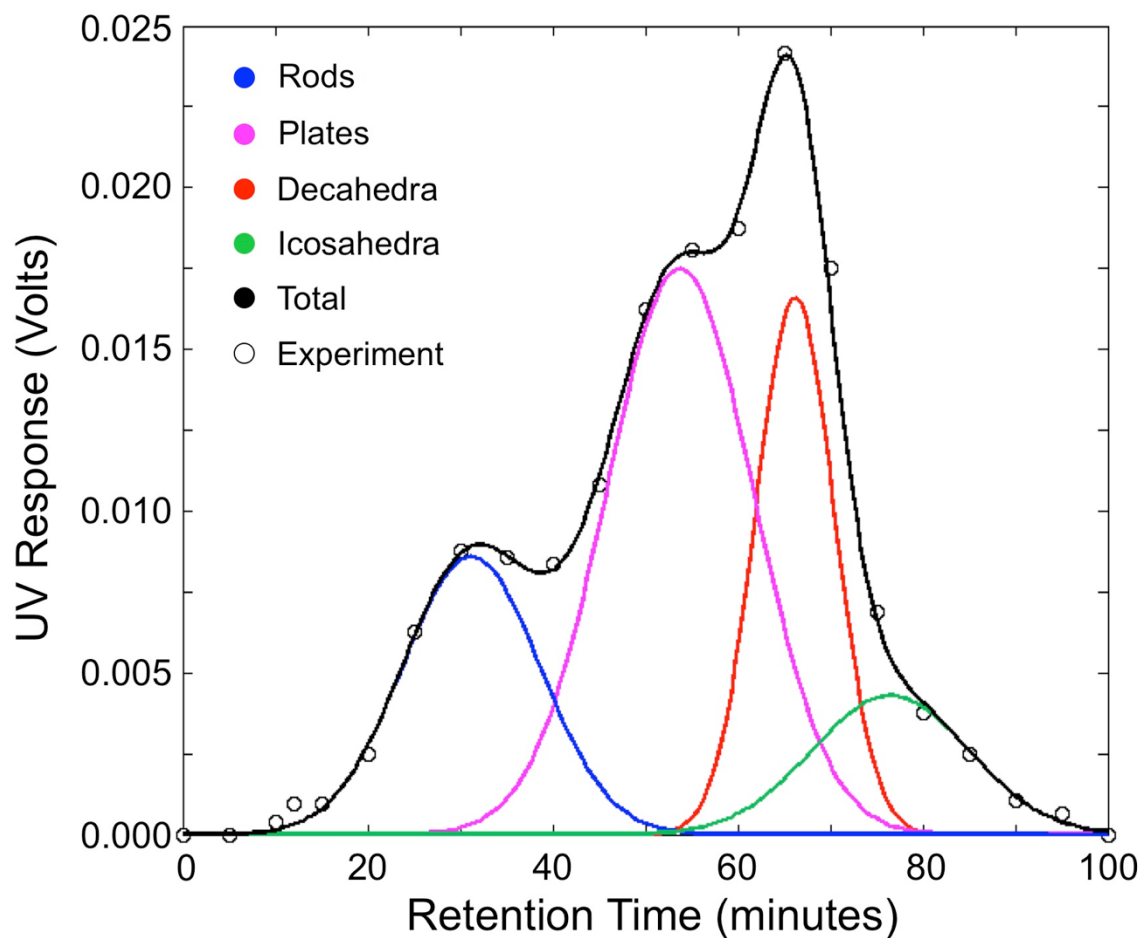


Figure S7. Separation of product morphologies. a, Centrifugal split-flow thin (C-SPLITT; performed by Postnova Analytics, Inc.) separation was performed on a representative sample mixture of nanorods, nanoplates, decahedra, and icosahedra. The eluent fractions were analyzed by TEM, revealing that the particles eluted in the order rods, plates, decahedra, icosahedra.

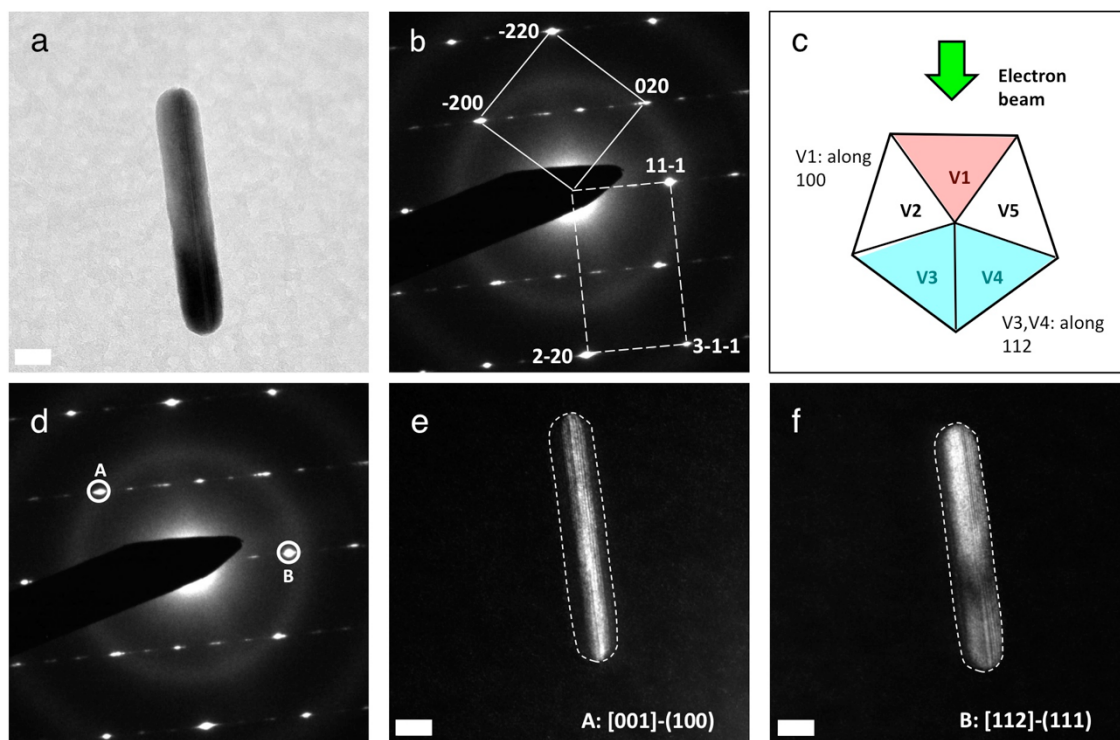


Figure S8. Evidence for five-fold structure of gold nanorods produced by the H_2O_2 -mediated synthesis. **a**, HRTEM of gold nanorod prepared by our approach. **b**, Electron diffraction pattern of nanorod in (a) demonstrating a superposition of [100] and [112] contributions. **c**, The electron beam is incident upon the nanorod as depicted in the schematic. **d**, Selected area electron diffraction pattern of nanorod in (a). The point labeled A corresponds to the [100] orientation and the point labeled B corresponds to the [112] orientation. **e**, The view along [100] produces strong contrast confined near the central axis of the rod, as expected from cross-section of the V1 tetrahedral subunit of the five-fold twinned structure. Dashed outline is included for clarity. **f**, The view along [112] produces strong contrast throughout the nanorod, as expected from the combined V3 and V4 tetrahedral subunits. These results provide strong evidence of the five-fold twin nanorod structure. Scale bar in (a) is 10 nm.

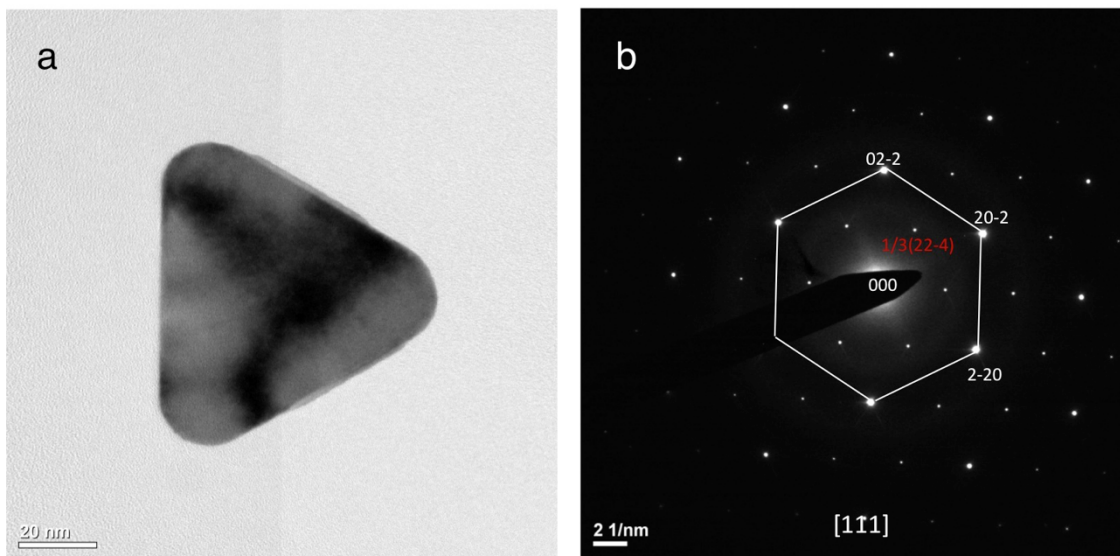


Figure S9. Electron diffraction of gold nanoplates. Electron diffraction analysis of the nanoplates reveals a forbidden $1/3\{22\bar{4}\}$ reflection, indicating the presence of twin planes parallel to the top and bottom $\{111\}$ facets. The electron diffraction pattern shown here corresponds to the nanoplate on the left. Several plates were analyzed and all demonstrated the forbidden reflection.

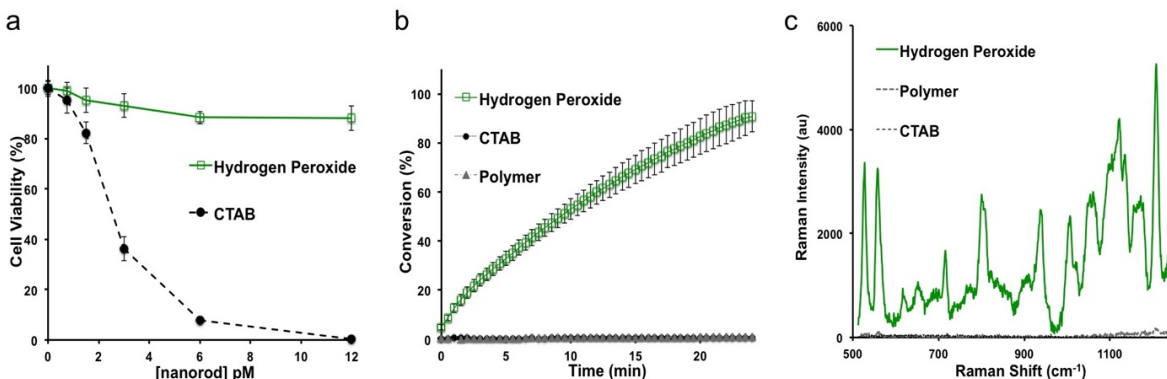


Figure S10. Comparison between our gold nanoparticles (hydrogen peroxide) and surfactant- and polymer-coated gold nanoparticles (CTAB and PEG-SH). a-c, We compared the (a) cytotoxicity, (b) catalytic activity (oxidation of resazurin to resorufin), and (c) surface-enhanced Raman scattering (dye = IR-792) capabilities of gold nanoparticles synthesized by our method to conventionally-prepared nanoparticles (comparable dimensions) with surfactant (CTAB) and thiolated polyethylene glycol (polymer) coatings. All nanoparticle mixtures were grown from the same seeds and comprised roughly 20% rods, 20% plates, and 60% pseudospherical nanoparticles. Nanoparticle aggregation did not occur under the low dye concentrations employed in these experiments. See methods for details.

Part II. Supplementary Movies

Supplementary Movie Details

Example videos of gold nanorod growth at different nucleation rates are provided in **Supplementary Movies 1-4** available for download in the Supporting Information online. The movies represent nucleation-limited growth with different ratios of {111} to {100} nucleation rates. The nucleation rates modeled in **Supplementary Movies 1-4** are, respectively, 1, 10, 100, and 1000 times faster on {111} facets than {100} facets.

Part III. Theoretical Framework

Overview of Theoretical Framework

Here we present a theoretical framework describing crystal growth originating from seed crystals exhibiting well-defined facets. Growth is assumed to begin with nucleation of a two-dimensional (2D) island and proceed by step flow (i.e. lateral growth) of the nucleus into a partial monolayer. The step flow is fueled by the incorporation of monomer growth units that adsorb onto the step and diffuse to binding sites. The completion of a net monolayer occurs when the 2D nucleus spreads a distance $\lambda = h_f - h_i$. If the surface is terraced, then multiple partial monolayers spread simultaneously and λ will be less than the length of the facet. The distance λ will also decrease as the number of 2D nuclei on a terrace increases. The goal of this theoretical framework is to develop an expression for facet growth rates (i.e. asymptotic growth rates) as a function of the expected time for 2D monolayer nucleation, the flux of growth units to the step front, and the jumping rates of adsorbed growth units. This rate expression can be used to determine the regimes of nucleation-limited, diffusion-limited, and reaction-limited growth.

Mathematical Approach

We determine the expected time for net monolayer completion – the time required for a facet to increase its average height by one monolayer – by summing the expected time for nucleation and the expected time for partial monolayer spread of a distance λ . The expected time for nucleation is treated as a known input, thus the primary calculation in this framework is the expected time for a step to become completely filled (henceforth called step completion).

The expected time for step completion is a function of the number of growth units in the step, the flux of growth units to the step front, and the activation energies for jumping into and along the step. In the following sections, we outline our theoretical framework by developing expressions for the expected times of growth unit arrival, one-dimensional (1D) step nucleation, and growth unit incorporation into binding sites. The latter process is divided into three separate mechanisms. The mechanism with the lowest expected time for step completion is defined to be the operating mechanism for the corresponding input parameters.

Expected Time of Growth Unit Arrival

Let the arrival of growth units at each site be modeled as a renewal process. Once growth units arrive at the step front, they diffuse into the step by a single jump. If the growth units are adsorbed on the surface, the rate at which they jump into the step is characterized by the vibrational frequency of the growth unit and activation energy of the jump. Growth units diffusing directly from solution into the step will have a different prefactor and activation energy than those corresponding to jumping into the step from a surface site. If the expected time for growth unit arrivals via diffusion, $E(T_{diff})$, is small compared to the expected time for jumps into the step, then the frequency of arrivals at each site can be well approximated by the asymptotic rate of the renewal process, R_{diff} :

$$R_{diff} = \frac{1}{E(T_{diff})}$$

Assuming that the expected time for growth unit arrival is constant along the step front, the arrival rate of growth units summed over x sites is xR_{diff} , and the expected arrival time is:

$$E(T_{diff})_x = \frac{1}{xR_{diff}}$$

When the arrival time is slow on the scale of incorporation into the step, it can be modeled as a rare event, which is well approximated by an exponential distribution. Such distributions have the characteristic relationship:

$$R_{diff} = \frac{1}{E(T_{diff})}$$

Which of course yields the same result for the expected arrival time over x sites:

$$E(T_{diff})_x = \frac{1}{xR_{diff}}$$

Let F denote the flux of growth units per nm per second to the step front, and let the length of a step unit, a_{\parallel} , be defined by the length, L , of the step and number, N , of growth units in the step:

$$F \equiv \text{flux in } \left(\frac{\text{units}}{\text{nm} \cdot \text{s}} \right)$$

$$a_{\parallel} = \frac{L}{N}$$

The flux of growth units per step site per second is

$$Fa_{\parallel} = \text{flux in } \left(\frac{\text{units}}{\text{site} \cdot \text{s}} \right)$$

Thus we have the following relation that holds for arrival times that are either small or large with respect to the expected time for jumping into the step:

$$E(T_{diff}) = \frac{1}{Fa_{\parallel}}$$

$$E(T_{diff})_x = \frac{1}{xFa_{\parallel}}$$

In this theoretical framework, we assume for simplicity that the expected time for growth unit arrival is well approximated by the reciprocal of the rate of growth unit arrival throughout the entire range of input flux values considered.

We are particularly interested in seeded (nano)crystal syntheses that proceed via reduction of a metal precursor by a weak reducing agent. Such syntheses are autocatalytic wherein the seed surface plays an essential role in catalyzing the reduction of metal atom precursors. In the present treatment, therefore, we will consider the rate of direct growth unit diffusion from solution into binding sites as negligible, since they must first interact with the surface before converting to the atomic form that is ultimately incorporated into the crystal. Application of this theory to systems wherein the direct diffusion from solution into binding sites is not negligible require modification of the equation for $E(T_{diff})_x$ to incorporate solution-to-binding site flux.

Expected Time of 1D Nucleation

The binding of a growth unit into an empty step is herein considered to constitute the process of one-dimensional (1D) nucleation. The term nucleation in this context refers to the beginning of 1D growth (i.e. along the step), rather than the attainment of a thermodynamic critical nucleus. Because a growth unit adsorbed to a step can detach before bonding to additional growth units in the step, it is important to consider whether or not the detachment rate should be used to modify the expected time for 1D nucleation. When the incorporation rate of a second growth unit is fast (e.g. more than an order of magnitude larger) with respect to the detachment of the first growth unit, the detachment rate can be neglected to a good approximation.

Let $E(T_{diff})_x$ denote the expected time for a growth unit to arrive at any one of x sites one jump away from a step site. The expected time for 1D nucleation will be a function of both $E(T_{diff})_x$ and the expected time for a growth unit to jump into a step site. Because a single surface jump is characterized by a large number of attempts (vibrational motion) and a low probability of success during each attempt, we can treat jumps into step sites as Poisson processes. As such, they are exponentially distributed, and the expected time of the process equals the reciprocal of the jump rate.

The Arrhenius rate, R_{Arrh} , of a surface diffusion process is given by:

$$R_{Arrh} = \nu_{ij} e^{-\frac{E_{ij}}{\kappa T}}$$

Where ν_{ij} is the component of vibrational frequency of the growth unit along the ij -direction, E_{ij} is the activation energy for jumping from i to j , κ is Boltzmann's constant, and T is the absolute temperature. If the jump is defined to occur in a particular direction, then an additional factor, p_{ij} , must be included to account for the probability of jumping in the direction of interest:

$$R_{ij} = p_{ij} \nu_{ij} e^{-\frac{E_{ij}}{\kappa T}}$$

For surface jumps, p_{ij} is well approximated as the reciprocal of the number of lattice sites that an adatom can reach in a single jump (e.g. $p_{ij} = 1/3$ for $\{111\}$ and $1/4$ for $\{100\}$, etc.}. The expected time for a single jump is therefore:

$$E(T_1)_{ij} = \frac{1}{R_{ij}}$$

$$E(T_1)_{ij} = \left(p_{ij} \nu_{ij} e^{-\frac{E_{ij}}{\kappa T}} \right)^{-1}$$

Let the subscripts L , U , K , and S denote the lower terrace, upper terrace, kink, and non-kink step sites, respectively. The expected time, $E(T_l)$, for jumps from the lower and upper terraces to the kink and non-kink step sites are given by:

$$E(T_1)_{LK} = \frac{1}{R_{LK}}$$

$$E(T_1)_{UK} = \frac{1}{R_{UK}}$$

$$E(T_1)_{LS} = \frac{1}{R_{LS}}$$

$$E(T_1)_{US} = \frac{1}{R_{US}}$$

Let P_j denote the probability that a growth unit arriving at the step front lands in site j , and let $E(T_{step}|j)$ denote the expected time for a growth unit to jump from site j into the adjacent step site, provided the growth unit arrives at site j . The expected time for 1D nucleation is given by:

$$E(T_{1D}) = E(T_{diff})_x + \sum_{j=1}^x P_j E(T_{step}|j)$$

When the probability of arriving at each site j is equal and growth units arrive from both the upper and lower terraces, this becomes:

$$E(T_{1D}) = E(T_{diff})_x + \frac{1}{2} \left(\frac{1}{R_{LS}} + \frac{1}{R_{US}} \right)$$

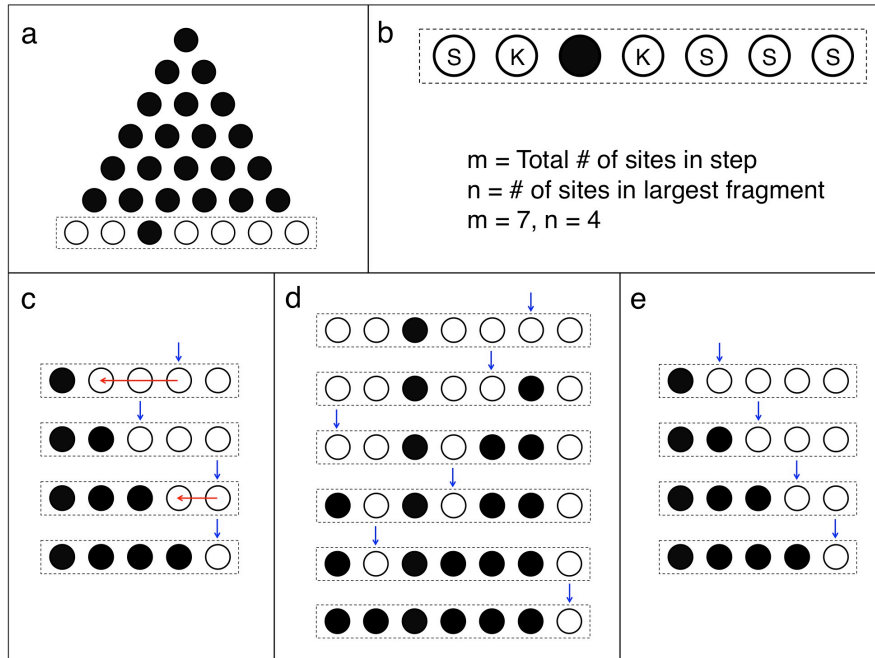


Figure TF1 | Growth Unit Incorporation at the Step Front. **a**, 1D nucleation at the edge of a triangular partial monolayer. The filled and unfilled circles represent occupied and unoccupied sites, respectively. **b**, Expanded view of the incomplete step in **a**. The sites labeled “k” are kink binding sites and those labeled “s” are non-kink step sites. The variables “m” and “n” are highlighted, which respectively denote the total number of sites in a step and the number of sites in the largest unfilled fragment. **c**, Mechanism 1 – Step adsorption and diffusion to kink. Growth units jump into the step (blue arrows) at random locations and diffuse along the step (red arrows) until they bind at the kink site. The non-kink step sites are modeled as a continuous time Markov chain to determine the expected time of step diffusion to the kink binding site. **d**, Mechanism 2 – Direct step incorporation. In contrast to Mechanism 1, this Mechanism 2 does not involve step diffusion. Mechanism 2 operates when the rate of step diffusion is slower than the rate of additional growth unit arrivals into the step sites. **e**, Mechanism 3 – Direct kink incorporation. Similar to Mechanism 2, Mechanism 3 does not involve step diffusion. In contrast to mechanisms 1 and 2, growth by Mechanism 3 occurs exclusively by jumps from the terrace to kink binding sites. This mechanism operates when the rate of step diffusion is slower than the rate of additional growth unit arrivals and the activation energy for jumping into kink sites is significantly lower than for jumping into non-kink step sites.

Expected Time of Incorporation – Step Adsorption and Diffusion

Let m denote the total number of step sites at the edge of a partial monolayer, as illustrated in **Figure TF1a,b**:

$$m \equiv \text{number of step sites}$$

The number of sites one jump from the step is a function of the facet index and step structure. Herein, we assume without loss of generality that there are $2m$ sites one jump away from step sites, corresponding to m sites on both the lower and upper terraces:

$$2m = \text{number of sites one jump away}$$

Upon 1D nucleation, the step is fragmented into segments of length less than m on either side of the incorporated growth unit (i.e. the 1D nucleus). Because step completion proceeds independently on either side of the 1D nucleus, the expected time for step completion equals the expected time for completion of the largest fragment. We denote the number of sites in the largest fragment by n (**Fig TF1b**). Given a step comprising m available sites for 1D nucleation, if a growth unit adsorbs at site $j \in (1, 2, \dots, m)$, n is defined as:

$$n = \text{maximum}(m - j, j - 1)$$

The step fragment comprises one kink binding site – the site adjacent to the 1D nucleus – and $n-1$ non-kink step sites. When the expected time for step diffusion to the kink binding site is less than the expected time for an additional growth unit to jump into the step we can model the step diffusion process by a continuous time Markov chain (CTMC). In particular, we construct an $(n-1) \times (n-1)$ *infinitesimal generator* matrix, typically called a *Q-matrix*. The Q-matrix, taken here to be positive dominant, has the form:

$$\mathbf{Q} = \begin{array}{c} \left| \begin{array}{cccccccc} R_1 & -R_{1,2} & 0 & 0 & 0 & 0 & 0 & 0 \\ -R_{2,1} & R_2 & -R_{2,3} & 0 & 0 & 0 & 0 & 0 \\ 0 & -R_{3,2} & R_3 & -R_{3,4} & 0 & 0 & 0 & 0 \\ 0 & 0 & -R_{4,3} & R_4 & -R_{4,5} & 0 & 0 & 0 \\ 0 & 0 & 0 & -R_{5,4} & R_5 & -R_{5,6} & 0 & 0 \\ 0 & 0 & 0 & 0 & -R_{6,5} & R_6 & -R_{6,7} & 0 \\ 0 & 0 & 0 & 0 & 0 & -R_{7,6} & R_7 & -R_{7,8} \\ 0 & 0 & 0 & 0 & 0 & 0 & -R_{8,7} & R_8 \end{array} \right| \end{array}$$

Where R_{ij} is the rate of jumping from i to j , and R_i is the total rate of jumping out of site i . Here we have arbitrarily chosen $n-1 = 8$ for illustrative purposes.

The expected time, $E(T_{bind})$, for a growth unit in a step to reach the binding site from each initial step site is obtained by inverting the Q-matrix, and summing the entries in each row:

$$\mathbf{ones}(n-1,1) = \begin{pmatrix} 1 \\ \vdots \\ 1 \end{pmatrix}$$

$$\mathbf{M} = \mathbf{Q}^{-1} \mathbf{ones}(n-1,1)$$

Entry $\mathbf{M}(j)$ gives the expected time of step diffusion to the binding site for a growth unit beginning in the step site j jumps from the kink binding site. The complete list of expected times to arrive at the binding site from any step site are given by the column vector $\mathbf{E}(T_{bind})$, where the first entry corresponds to a growth unit that is already in the binding site, the second entry corresponds to the position one jump away, and so on:

$$\mathbf{E}(T_{bind}) = \begin{bmatrix} 0 \\ \mathbf{M}(1) \\ \vdots \\ \mathbf{M}(n-1) \end{bmatrix}$$

The column vector of expected times for jumping from the terrace into each step site is given by:

$$\mathbf{E}(T_{step}) = \left(\frac{1}{2n} \right) \begin{bmatrix} \frac{1}{R_{L_0 S_0}} + \frac{1}{R_{U_0 S_0}} \\ \frac{1}{R_{L_1 S_1}} + \frac{1}{R_{U_1 S_1}} \\ \vdots \\ \frac{1}{R_{L_{n-1} S_{n-1}}} + \frac{1}{R_{U_{n-1} S_{n-1}}} \end{bmatrix}$$

Where the coefficient $1/2n$ is the probability that an atom impinging upon the step front arrives at the specific site L_j or U_j (e.g. if there are $2n = 18$ sites one jump away from the step, each has probability = $1/18$ that an impinging adatom arrives at that specific site). Here we have assumed that each site has equal likelihood of adatom arrival. For convenience, we construct a column vector with n entries, rather than $2n$, where each entry equals the sum of the contribution from the corresponding upper terrace and lower terrace sites. If the probability of growth unit arrival is different for lower terrace versus upper terrace sites then each site must be given its own entry and corresponding probability of arrival in the $\mathbf{E}(T_{step})$ column vector.

We determine the expected time of the growth unit incorporation reaction, $E(T_{rxn})$, by summing all entries in the two column vectors, $\mathbf{E}(T_{step})$ and $\mathbf{E}(T_{bind})$.

$$E(T_{step} + T_{bind}) = \left(\frac{1}{2n}\right) \begin{bmatrix} \frac{1}{R_{L_0S_0}} + \frac{1}{R_{U_0S_0}} \\ \frac{1}{R_{L_1S_1}} + \frac{1}{R_{U_1S_1}} \\ \vdots \\ \frac{1}{R_{L_{n-1}S_{n-1}}} + \frac{1}{R_{U_{n-1}S_{n-1}}} \end{bmatrix} + \left(\frac{1}{n}\right) \begin{bmatrix} 0 \\ M(1) \\ \vdots \\ M(n-1) \end{bmatrix}$$

$$\mathbf{ones}(1, n) = [1, 1, \dots, 1]$$

$$E(T_{rxn}) = \mathbf{ones}(1, n)E(T_{step} + T_{bind})$$

$$E(T_{rxn}) = [1, 1, \dots, 1] \begin{bmatrix} \left(\frac{1}{n}\right) \left\{ 0 + \frac{1}{2R_{L_0S_0}} + \frac{1}{2R_{U_0S_0}} \right\} \\ \left(\frac{1}{n}\right) \left\{ M(1) + \frac{1}{2R_{L_1S_1}} + \frac{1}{2R_{U_1S_1}} \right\} \\ \vdots \\ \left(\frac{1}{n}\right) \left\{ M(n-1) + \frac{1}{2R_{L_{n-1}S_{n-1}}} + \frac{1}{2R_{U_{n-1}S_{n-1}}} \right\} \end{bmatrix}$$

Given a flux of F atoms per nm per second to the step front, the expected time for adatom arrival is:

$$E(T_{diff})_{2n} = \frac{1}{2na_{\parallel}F}$$

Thus, the expected time for attachment of an adatom to a kink site in a step fragment of length n is:

$$E(t_{att})_n = E(T_{diff})_{2n} + E(T_{rxn})$$

The expected time for growth unit incorporation, $E(T_{inc})$, must correct for the detachment rate, R_{det} , of atoms during growth. We do this by adding the correction factor, CF :

$$CF = \left\{ \frac{\frac{1}{R_{det}}}{\left[\frac{1}{R_{det}} - E(t_{att}) \right]} \right\}$$

The derivation of the correction factor is provided at the end of the theoretical framework. For the example of adatoms approaching a step from the upper and lower terraces, the correction factor takes the form:

$$CF = \left\{ \frac{(R_{KL})^{-1}}{(R_{KL})^{-1} - [E(T_{diff})_{2n} + E(T_{rxn})]} \right\}$$

$$E(T_{inc}) = CF \left\{ E(T_{diff})_{2n} + \mathbf{ones}(1, k) [E(T_{step} + T_{bind})_k] \right\}$$

The expected time for step fragment completion, $E(T_{fragment})$, is obtained repeating the calculation of $E(T_{inc})$ after each new atom is added into the step until all sites have been filled:

$$E(T_{fragment}) = \sum_{k=1}^n E(T_{inc})_k$$

$$E(T_{fragment}) = \sum_{k=1}^n CF_k \left\{ E(T_{diff})_{2k} + \mathbf{ones}(1, k) [E(T_{step} + T_{bind})_k] \right\}$$

The term $E[(T_{step} + T_{bind})_k]$ varies depending upon the mechanism of adatom incorporation, and thus must be explicitly defined. Because the 1D nucleation event can occur at any one of the m available sites, we must randomize the initial growth unit adsorption in order to arrive at the expected time for step completion. The resulting equation gives the expected time for completion of an entire row (i.e. entire step), $E(T_{row})$, according to the mechanism depicted in **Figure TF1c**:

$$E(T_{row})_{mech.1} = \left[E(T_{diff})_{2m} + \frac{1}{2R_{LS}} + \frac{1}{2R_{US}} \right] + \frac{1}{m} \sum_{j=1}^m \sum_{k=1}^n E(T_{inc})_k$$

$$E(T_{step} + T_{bind})_{k=1} = \frac{1}{2} \left(\frac{1}{R_{LK}} + \frac{1}{R_{UK}} \right)$$

$$E(T_{step} + T_{bind})_{k=2} = \left[\frac{1}{4} \left(\frac{1}{R_{LK}} + \frac{1}{R_{UK}} \right) \right. \\ \left. \frac{1}{4} \left(\frac{1}{R_{LS}} + \frac{1}{R_{US}} + \frac{2}{R_{SK}} \right) \right]$$

$$E(T_{step} + T_{bind})_{k \geq 3} = \left(\frac{1}{k} \right) \left[\begin{array}{c} \frac{1}{2} \left(\frac{1}{R_{LK}} + \frac{1}{R_{UK}} \right) \\ M(1) + \frac{1}{2} \left(\frac{1}{R_{LS}} + \frac{1}{R_{US}} \right) \\ \vdots \\ M(k-1) + \frac{1}{2} \left(\frac{1}{R_{LS}} + \frac{1}{R_{US}} \right) \end{array} \right]$$

Recall that $n = \text{maximum}(m-j, j-1)$

Expected Time of Incorporation – Direct Step Binding

When the arrival of growth units into the step becomes sufficiently fast, the mechanism of incorporation no longer includes diffusion along the step (**Fig TF1d**). In general, these conditions have sufficiently fast growth rates such that the approximation $CF \approx 1$ tends to be very good (i.e., kink detachment rates are negligible). For this reason, we have omitted the correction factor from the $E(T_{row})$ equations, but this approximation should be verified whenever running the theoretical framework on a new system. The threshold where the incorporation mechanism changes from step adsorption and diffusion to direct step binding (i.e. incorporation without diffusion within the step) can be approximated by comparing the expected time for growth units to jump into the step and the expected time for growth units to diffuse to the kink. In particular, the mechanism changes when the expected time for a growth unit to diffuse to a kink is greater than the expected time for a second growth unit to jump into the step.

The expected time to complete a row of step atoms, $E(T_{row})$, via direct step binding is determined by summing the expected times for consecutive arrival and step adsorption events. For a step with m available binding sites prior to 1D nucleation we have:

$$E(T_{row})_{mech.2} = \sum_{k=0}^{m-1} E(T_{diff})_{2(m-k)} + \frac{1}{2} \left(\frac{1}{R_{LS}} + \frac{1}{R_{US}} \right)_k$$

Where the subscript k on the last term indicates that the expected time for jumping into the step can change as the number of adsorbed growth units in the step changes. When the activation energy for incorporation into the step does not depend strongly on the number of adsorbed growth units then the following approximation can be used:

$$E(T_{row})_{mech.2} = \sum_{k=0}^{m-1} E(T_{diff})_{2(m-k)} + \left(\frac{m}{2} \right) \left(\frac{1}{R_{LS}} + \frac{1}{R_{US}} \right)$$

Note that because the step does not complete symmetrically outward from the 1D nucleation site it is not sufficient to consider only the completion of the largest step fragment of n sites. Notice also that the detachment rate has been neglected because step completion occurs very rapidly with respect to growth unit detachment.

Expected Time of Incorporation – Direct Kink Binding

As the expected time for growth unit arrival at the step front approaches zero, incorporation into the step becomes reaction limited. When the activation energy for direct incorporation into a kink site is significantly lower than that for direct incorporation into a non-kink step site, the minimum expected time for step completion will occur via direct kink binding (**Fig TF1e**). That is, after 1D nucleation, growth units will exclusively incorporate into the step by jumping from the terraces into the kink

binding sites. Because this mechanism creates symmetric kink propagation from the initial 1D nucleation site, the expected time for step completion equals the expected time for the largest step fragment of n sites. Thus, the expected time equals the expected time for 1D nucleation randomized over the m possible nucleation sites plus the expected time for n consecutive kink binding events:

$$E(T_{row})_{mech.3} = \left[E(T_{diff})_{2m} + \frac{1}{2R_{LS}} + \frac{1}{2R_{US}} \right] + \frac{1}{m} \sum_{j=1}^m \left\{ n \left[E(T_{diff})_2 + \frac{1}{2} \left(\frac{1}{R_{LK}} + \frac{1}{R_{UK}} \right) \right] \right\}$$

$$n = \text{maximum}(m - j, j - 1)$$

Expected Time of Step Completion

The expected time to complete a row of step atoms is a function of the incorporation mechanism and flux of growth units to the step front, as described above. Here we present the six step completion equations: the three growth mechanisms from above, each with an expression for a system wherein growth units arrive from the lower and upper terraces and a system wherein growth units arrive exclusively from the lower terrace. If the expected time for step diffusion to kink binding sites is less than the expected time for a second growth unit to jump into the step, then mechanism 1 (i.e. step adsorption and diffusion) is used. Otherwise, the expected time for step completion via mechanisms 2 and 3 are both computed and the minimum expected time is selected. This process is repeated from the initial step – corresponding to the edge of the 2D critical nucleus – to the final step, defined as the step that completes a net monolayer.

The six expressions considered are summarized below:

Mechanism 1, Upper and Lower Terrace

$$E(T_{row})_{mech.1} = \left[E(T_{diff})_{2m} + \frac{1}{2R_{LS}} + \frac{1}{2R_{US}} \right] + \frac{1}{m} \sum_{j=1}^m \sum_{k=1}^n E(T_{inc})_k$$

$$E(T_{step} + T_{bind})_{k=1} = \frac{1}{2} \left(\frac{1}{R_{LK}} + \frac{1}{R_{UK}} \right)$$

$$E(T_{step} + T_{bind})_{k=2} = \left[\frac{1}{4} \left(\frac{1}{R_{LK}} + \frac{1}{R_{UK}} \right) \right] + \left[\frac{1}{4} \left(\frac{1}{R_{LS}} + \frac{1}{R_{US}} + \frac{2}{R_{SK}} \right) \right]$$

$$E(T_{step} + T_{bind})_{k \geq 3} = \left(\frac{1}{k}\right) \begin{bmatrix} \frac{1}{2} \left(\frac{1}{R_{LK}} + \frac{1}{R_{UK}} \right) \\ M(1) + \frac{1}{2} \left(\frac{1}{R_{LS}} + \frac{1}{R_{US}} \right) \\ \vdots \\ M(k-1) + \frac{1}{2} \left(\frac{1}{R_{LS}} + \frac{1}{R_{US}} \right) \end{bmatrix}$$

Mechanism 1, Lower Terrace Only

$$E(T_{row})_{mech.1L} = \left[E(T_{diff})_m + \frac{1}{R_{LS}} \right] + \frac{1}{m} \sum_{j=1}^m \sum_{k=1}^n E(T_{inc})_k$$

$$E(T_{step} + T_{bind})_{k=1} = \frac{1}{R_{LK}}$$

$$E(T_{step} + T_{bind})_{k=2} = \left[\begin{array}{c} \frac{1}{2R_{LK}} \\ \frac{1}{2} \left(\frac{1}{R_{LS}} + \frac{1}{R_{SK}} \right) \end{array} \right]$$

$$E(T_{step} + T_{bind})_{k \geq 3} = \left(\frac{1}{k}\right) \begin{bmatrix} \frac{1}{R_{LK}} \\ M(1) + \frac{1}{R_{LS}} \\ \vdots \\ M(k-1) + \frac{1}{R_{LS}} \end{bmatrix}$$

Mechanism 2, Upper and Lower Terrace

$$E(T_{row})_{mech.2} = \sum_{k=0}^{m-1} E(T_{diff})_{2(m-k)} + \left(\frac{m}{2}\right) \left(\frac{1}{R_{LS}} + \frac{1}{R_{US}} \right)$$

Mechanism 2, Lower Terrace Only

$$E(T_{row})_{mech.2L} = \sum_{k=0}^{m-1} E(T_{diff})_{(m-k)} + \frac{m}{R_{LS}}$$

Mechanism 3, Upper and Lower Terrace

$$E(T_{row})_{mech.3} = \left[E(T_{diff})_{2m} + \frac{1}{2R_{LS}} + \frac{1}{2R_{US}} \right] + \frac{1}{m} \sum_{j=1}^m \left\{ n \left[E(T_{diff})_2 + \frac{1}{2} \left(\frac{1}{R_{LK}} + \frac{1}{R_{UK}} \right) \right] \right\}$$

$$n = \text{maximum}(m - j, j - 1)$$

Mechanism 3, Lower Terrace Only

$$E(T_{row})_{mech.3L} = \left[E(T_{diff})_m + \frac{1}{R_{LS}} \right] + \frac{1}{m} \sum_{j=1}^m \left\{ n \left[E(T_{diff})_1 + \frac{1}{R_{LK}} \right] \right\}$$

$$n = \text{maximum}(m - j, j - 1)$$

Formula for Step Size as a Function of Partial Monolayer Radius

In order to employ the expected time for step completion to determine the expected time for layer completion, we must derive an expression for the number of step sites as a function of the partial monolayer size. If we consider step flow via the completion of consecutive single steps, then the geometry of the partial monolayer and the symmetry of its growth (e.g. a triangle growing from three edges, a triangle growing from one edge, etc.) will be the primary factors in developing an expression for the number of step sites, $m(h)$, as a function of the length, h , of the partial monolayer. Because we are especially interested in growth originating from the corners of triangular $\{111\}$ facets (i.e. symmetry of growth on $\{111\}$ nanorod facets), we will use the expression for a triangular partial monolayer growing from one edge:

$$m(h + 1) = m(h) + 1$$

When alternative geometries and growth symmetries are used, the appropriate expression is likely to change. The form of the recursion formula will only change by the value of the constant for many relevant cases.

Expected Time of Net Monolayer Completion

Once the expected time for step completion and the formula for the number of step sites as a function of partial monolayer size are known, the expected time of net monolayer completion is straightforward to compute. Using the example of a triangular partial monolayer spreading from one edge, we can see that the m^{th} step requires m growth units for completion. We can therefore determine the expected time for monolayer completion by summing the expected time for step completion over the total number of steps required to complete a net monolayer:

Mechanism 1, Upper and Lower Terrace

$$E(T_{monolayer})_{mech.1} = \sum_{m=h_i}^{h_f} \left[E(T_{diff})_{2m} + \frac{1}{2} \left(\frac{1}{R_{LS}} + \frac{1}{R_{US}} \right) + \frac{1}{m} \sum_{j=1}^m \sum_{k=1}^n E(T_{inc})_k \right]$$

$$E(T_{step} + T_{bind})_{k=1} = \frac{1}{2} \left(\frac{1}{R_{LK}} + \frac{1}{R_{UK}} \right)$$

$$E(T_{step} + T_{bind})_{k=2} = \left[\begin{array}{c} \frac{1}{4} \left(\frac{1}{R_{LK}} + \frac{1}{R_{UK}} \right) \\ \frac{1}{4} \left(\frac{1}{R_{LS}} + \frac{1}{R_{US}} + \frac{2}{R_{SK}} \right) \end{array} \right]$$

$$E(T_{step} + T_{bind})_{k \geq 3} = \left(\frac{1}{k} \right) \left[\begin{array}{c} \frac{1}{2} \left(\frac{1}{R_{LK}} + \frac{1}{R_{UK}} \right) \\ M(1) + \frac{1}{2} \left(\frac{1}{R_{LS}} + \frac{1}{R_{US}} \right) \\ \vdots \\ M(k-1) + \frac{1}{2} \left(\frac{1}{R_{LS}} + \frac{1}{R_{US}} \right) \end{array} \right]$$

Mechanism 1, Lower Terrace Only

$$E(T_{monolayer})_{mech.1L} = \sum_{m=h_i}^{h_f} \left\{ \left[E(T_{diff})_m + \frac{1}{R_{LS}} \right] + \frac{1}{m} \sum_{j=1}^m \sum_{k=1}^n E(T_{inc})_k \right\}$$

$$E(T_{step} + T_{bind})_{k=1} = \frac{1}{R_{LK}}$$

$$E(T_{step} + T_{bind})_{k=2} = \left[\begin{array}{c} \frac{1}{2R_{LK}} \\ \frac{1}{2} \left(\frac{1}{R_{LS}} + \frac{1}{R_{SK}} \right) \end{array} \right]$$

$$E(T_{step} + T_{bind})_{k \geq 3} = \left(\frac{1}{k} \right) \begin{bmatrix} \frac{1}{R_{LK}} \\ M(1) + \frac{1}{R_{LS}} \\ \vdots \\ M(k-1) + \frac{1}{R_{LS}} \end{bmatrix}$$

Mechanism 2, Upper and Lower Terrace

$$E(T_{monolayer})_{mech.2} = \sum_{m=h_i}^{h_f} \left[\sum_{k=0}^{m-1} E(T_{diff})_{2(m-k)} + \left(\frac{m}{2} \right) \left(\frac{1}{R_{LS}} + \frac{1}{R_{US}} \right) \right]$$

Mechanism 2, Lower Terrace Only

$$E(T_{monolayer})_{mech.2L} = \sum_{m=h_i}^{h_f} \left[\sum_{k=0}^{m-1} E(T_{diff})_{(m-k)} + \frac{m}{R_{LS}} \right]$$

Mechanism 3, Upper and Lower Terrace

$$E(T_{monolayer})_{mech.3} = \sum_{m=h_i}^{h_f} \left[\left(E(T_{diff})_{2m} + \frac{1}{2R_{LS}} + \frac{1}{2R_{US}} \right) + \frac{1}{m} \sum_{j=1}^m \left\{ n \left[E(T_{diff})_2 + \frac{1}{2} \left(\frac{1}{R_{LK}} + \frac{1}{R_{UK}} \right) \right] \right\} \right]$$

$$n = \text{maximum}(m - j, j - 1)$$

Mechanism 3, Lower Terrace Only

$$E(T_{monolayer})_{mech.3L} = \sum_{m=h_i}^{h_f} \left(\left[E(T_{diff})_m + \frac{1}{R_{LS}} \right] + \frac{1}{m} \sum_{j=1}^m \left\{ n \left[E(T_{diff})_1 + \frac{1}{R_{LK}} \right] \right\} \right)$$

$$n = \text{maximum}(m - j, j - 1)$$

Asymptotic Growth Rate Normal to Surface

Although the expected time for net monolayer completion has a clear meaning and strong mathematical foundation, it is much more common to experimentally measure and report crystal growth “rates”. Although the rate of a process has an intuitive colloquial meaning, it is important to articulate exactly which rate is referenced when attempting to provide a meaningful mathematical expression. Because there is no reason to assume that the time for monolayer completion should be an exponentially distributed random variable, it cannot be assumed that the “rate” of monolayer completion is defined as the reciprocal of the expected time for monolayer completion. It is, however, reasonable to consider the asymptotic rate of monolayer formation over growth of several tens of nanometers. In this case, we can treat monolayer formation as a renewal process, and thus the expected time for layer formation as constant. This requires that we assume that the expected time for nucleation and the flux of growth units per step site per second are constant throughout the timeframe of crystal growth. Note, however, that a seed crystal growing from time t_1 to t_2 and another seed crystal growing from time t_3 to t_4 can be subject to different nucleation rates and flux. The (asymptotic) rate of crystal growth, R_{hkl} , normal to a facet with Miller indices hkl and monolayer height d_{hkl} is defined as:

$$R_{hkl} = \frac{d_{hkl}}{E(T_{monolayer})_{hkl}}$$

The units of R_{hkl} are nm per second, and the logarithm of this rate as a function of nucleation rate and growth unit flux is used to generate the crystal growth contour plots reported in the main text. The advantage of using this expression is that it can be compared to experimental measurements and alternative rate expressions commonly found in the literature. It should be noted, however, that working instead with the expected time for monolayer formation provides the advantages of a slightly less restricted mathematical foundation and distinct contributions from the expected times of 2D nucleation and partial monolayer spread.

Derivation of the Correction Factor for the Detachment of Growth Units

Suppose we want to know the expected time for a step fragment of n unfilled sites to be completely filled, one site at a time. If the expected time for one atom to fill a binding site is $E(t_{att})$, then the expected time, $E(t_{n,att})$, for n binding events is:

$$E(t_{n,att}) = nE(t_{att})$$

If detachment of atoms from binding sites did not occur, then $E(t_n)$ would be the expected time for the step fragment comprising n atoms to be completed. In reality, however, atoms detach from binding sites at a rate of R_{det} . Because the detachment is a Poisson process, the expected time for an atom to detach, $E(t_{det})$, is:

$$E(t_{det}) = \frac{1}{R_{det}}$$

From the expected times for incorporation and detachment of atoms at binding sites, we can write the expected number of attachments, N_{att} , and detachments, N_{det} , from time $t = 0$ to τ :

$$N_{att}(\tau) = \frac{\tau}{E(t_{att})}$$

$$N_{det}(\tau) = \frac{\tau}{E(t_{det})}$$

The number of attachments minus the number of detachments gives the net number of atoms incorporated, N_{inc} . The net number of atoms incorporated in time τ , is:

$$N_{inc}(\tau) = N_{att}(\tau) - N_{det}(\tau)$$

$$N_{inc}(\tau) = \frac{\tau}{E(t_{att})} - \frac{\tau}{E(t_{det})}$$

$$N_{inc}(\tau) = \frac{\tau[E(t_{det}) - E(t_{att})]}{E(t_{att})E(t_{det})}$$

Setting $\tau = 1s$ gives the net number of atoms incorporated per second:

$$N_{inc} \left(\frac{atoms}{s} \right) = \frac{[E(t_{det}) - E(t_{att})]}{E(t_{att})E(t_{det})}$$

In order to determine the expected time, in seconds, for an atom to be incorporated, $E(t_{inc})$, we take the reciprocal of N_{inc} :

$$E(t_{inc}) = \frac{1}{N_{inc}}$$

$$E(t_{inc}) = \frac{E(t_{att})E(t_{det})}{[E(t_{det}) - E(t_{att})]}$$

$$E(t_{inc}) = \left\{ \frac{E(t_{det})}{[E(t_{det}) - E(t_{att})]} \right\} E(t_{att})$$

The expected time, $E(t_{n,inc})$, for n sites to be filled (i.e. $N_{att} - N_{det} = n$), is therefore given by:

$$E(t_{n,inc}) = nE(t_{inc})$$

$$E(t_{n,inc}) = \left\{ \frac{E(t_{det})}{[E(t_{det}) - E(t_{att})]} \right\} nE(t_{att})$$

We see in the last expression, that the net time for n sites to be filled is equal to n times the expected time of attachment, multiplied by the ratio

$$\left\{ \frac{E(t_{det})}{[E(t_{det}) - E(t_{att})]} \right\} = \left\{ \frac{\frac{1}{R_{det}}}{\left[\frac{1}{R_{det}} - E(t_{att}) \right]} \right\}$$

Alternatively, we can derive this factor from the rates of attachment, detachment, and the net rate of incorporation:

$$R_{inc} = R_{att} - R_{det}$$

If we assume that the incorporation of growth units is well modeled by a renewal process wherein the asymptotic rate of attachment gives a good approximation to the experimental rate of attachment, we can apply the theorem:

$$\lim_{t \rightarrow \infty} \frac{N_{att}}{t} = \frac{1}{E(t_{att})}$$

$$R_{att} = \frac{N_{att}}{t}$$

$$R_{att} = \frac{1}{E(t_{att})}$$

$$R_{inc} = \frac{1}{E(t_{att})} - R_{det}$$

Then the expected time for n sites to be filled is given by:

$$R_{inc} E(t_{n,inc}) = n$$

$$E(t_{n,inc}) = \frac{n}{R_{inc}}$$

$$E(t_{n,inc}) = \frac{n}{\left[\frac{1}{E(t_{att})} - R_{det} \right]}$$

$$E(t_{n,inc}) = \frac{n}{\left[\frac{1}{E(t_{att})} - \frac{1}{E(t_{det})} \right]}$$

$$E(t_{n,inc}) = \frac{n}{\left[\frac{E(t_{det}) - E(t_{att})}{E(t_{att})E(t_{det})} \right]}$$

$$E(t_{n,inc}) = \frac{E(t_{att})E(t_{det})n}{E(t_{det}) - E(t_{att})}$$

$$E(t_{n,inc}) = \left[\frac{E(t_{det})}{E(t_{det}) - E(t_{att})} \right] nE(t_{att})$$

Which again defines the expected time for incorporation as the expected time of attachment, multiplied by the ratio

$$\left\{ \frac{E(t_{det})}{[E(t_{det}) - E(t_{att})]} \right\} = \left\{ \frac{\frac{1}{R_{det}}}{\left[\frac{1}{R_{det}} - E(t_{att}) \right]} \right\}$$